THE JOURNAL OF BIOLOGICAL CHEMISTRY
Vol. 277, No. 37, Issue of September 13, pp. 34247–34253, 2002

Printed in U.S.A.

Pore Formation and Function of Phosphoporin PhoE of *Escherichia coli* Are Determined by the Core Sugar Moiety of Lipopolysaccharide*

Received for publication, February 27, 2002, and in revised form, June 11, 2002
Published, JBC Papers in Press, June 28, 2002, DOI 10.1074/jbc.M201950200

Sven O. Hagge‡, Hans de Cock§, Thomas Gutsmann‡, Frank Beckers§, Ulrich Seydel‡, and Andre Wiese‡¶

From the ‡Research Center Borstel, Center for Medicine and Biosciences, Department of Immunochemistry and Biochemical Microbiology, Parkallee 1-40, D-23845 Borstel, Germany and the §Department of Molecular Cell Biology, Institute for Biomembranes, Utrecht University, Padualaan 8, 3584 CH Utrecht, The Netherlands

The lipid matrix of the outer membrane of Gram-negative bacteria is an asymmetric bilayer composed of a phospholipid inner leaflet and a lipopolysaccharide outer leaflet. Incorporated into this lipid matrix are, among other macromolecules, the porins, which have a sieve-like function for the transport or exclusion of hydrophilic substances. It is known that a reduced amount of porins is found in the outer membrane of rough mutants as compared with wild-type bacteria. This observation was discussed to be caused by a reduced number of insertion sites in the former. We performed electrical measurements on reconstituted planar bilayers composed of lipopolysaccharide on one side and a phospholipid mixture on the other side using lipopolysaccharide from various rough mutant strains of *Salmonella enterica* serovar Minnesota. We found that pore formation by PhoE trimers that were added to the phospholipid side of the bilayers increased with the increasing length of the lipopolysaccharide core sugar moiety. These results allow us to conclude that the length of the sugar moiety of lipopolysaccharide is the parameter governing pore formation and that no particular insertion sites are required. Furthermore, we found that the voltage gating of the porin channels is strongly dependent on the composition of the lipid matrix.

The cell envelope of Gram-negative bacteria consists of the cytoplasmic membrane, the peptidoglycan layer, and an additional barrier, the outer membrane (OM),[1] (1) which is strictly asymmetric with respect to its lipid composition. Whereas the inner membrane (IM) is composed on both sides of phospholipids, the OM consists of a phospholipid inner leaflet and a lipopolysaccharide (LPS) outer leaflet. The LPS consists of an oligo- or polysaccharide portion covalently linked to a lipid component termed lipid A, which anchors the molecule in the membrane (2). In wild-type strains, the polysaccharide portion consists of an *O*-specific chain and the core oligosaccharide. Rough mutant strains do not express the *O*-specific chain, but retain core oligosaccharides of varying length. The LPS of various rough mutants are characterized by chemotypes in a sequence of decreasing length of the core sugar as Ra (complete core), Rb, Rc, Rd, and Re. Deep-rough LPS (Re LPS) represents the minimal structure of LPS consisting of only lipid A and two 3-deoxy-D-*manno*-oct-2-ulosonic acid (Kdo) monosaccharides (3) (Fig. 1).

The OM protects the cell from harmful agents like antibiotics and toxins and against changes in osmotic pressure. Transmembrane proteins, the porins, allowing the uptake and disposal of small hydrophilic compounds such as nutrients and waste products (4), are assembled in the OM. In *Escherichia coli* OmpF and OmpC represent the general diffusion pores. The phosphoporin PhoE is synthesized when cells are grown under phosphate limitation (5). PhoE has a molecular weight of M_r 36,822 and an exclusion size of M_r ~600 and is weakly anion selective (6). The crystal structure of PhoE has been solved (7). The channel-forming motif of PhoE is a 16-strand anti-parallel β-barrel. Short β-hairpin turns define the periplasmic end of the barrel, whereas long irregular loops are found at the cell surface. The functional unit of this protein is a trimer.

Outer membrane proteins are synthesized as precursor proteins in the cytoplasm. After their translocation across the IM via the Sec machinery (8) and processing to mature protein, they are assembled into the OM. The amino-terminal signal sequence is removed during or after translocation through the IM (9). It has been shown that Re mutants contain reduced amounts of PhoE (10) and other outer membrane proteins (11). From *in vitro* studies it is known that the efficiency of assembly of porins in the OM decreases from strains with an LPS with a complete core sugar moiety to those with an LPS with a short sugar moiety. For PhoE a decrease of 95% was found for a Re mutant in comparison to a Ra mutant (12). Furthermore, it has been shown in an *in vitro* model that the chemical structure and the biophysical properties of LPS are important for a correct and efficient folding of PhoE into a native-like, trimerization-competent, folded monomeric form (13). The folding of *in vitro* synthesized non-native PhoE protein into a native-like monomeric form was more efficient with LPS of chemotype Ra (Ra LPS) as compared to Re LPS, lacking a large part of the core. The absence or presence of a negative charge at the first heptose in the core region seemed to be of special importance in this respect. Also, the efficiency of folding and trimerization of OmpF porin *in vitro* was shown to depend on the LPS structure (14).

* This work was supported by the Deutsche Forschungsgemeinschaft, SFB 470, Project B5. The costs of publication of this article were defrayed in part by the payment of page charges. This article must therefore be hereby marked "*advertisement*" in accordance with 18 U.S.C. Section 1734 solely to indicate this fact.

¶ To whom correspondence should be addressed: Research Center Borstel, Center for Medicine and Biosciences, Dept. of Immunochemistry and Biochemical Microbiology, Parkallee 10 D-23845 Borstel, Germany. Tel.: 49-4537-188-291; Fax: 49-4537-188-632; E-mail: awiese@fz-borstel.de.

[1] The abbreviations used are: OM, outer membrane; IM, inner membrane; LPS, lipopolysaccharide; GSL-1, monosaccharide-type fraction of glycosphingolipid; PL, phospholipid mixture; PE, phosphatidylethanolamine; PG, phosphatidylglycerol; DPG, diphosphatidylglycerol; Kdo, 3-deoxy-D-*manno*-oct-2-ulosonic acid.

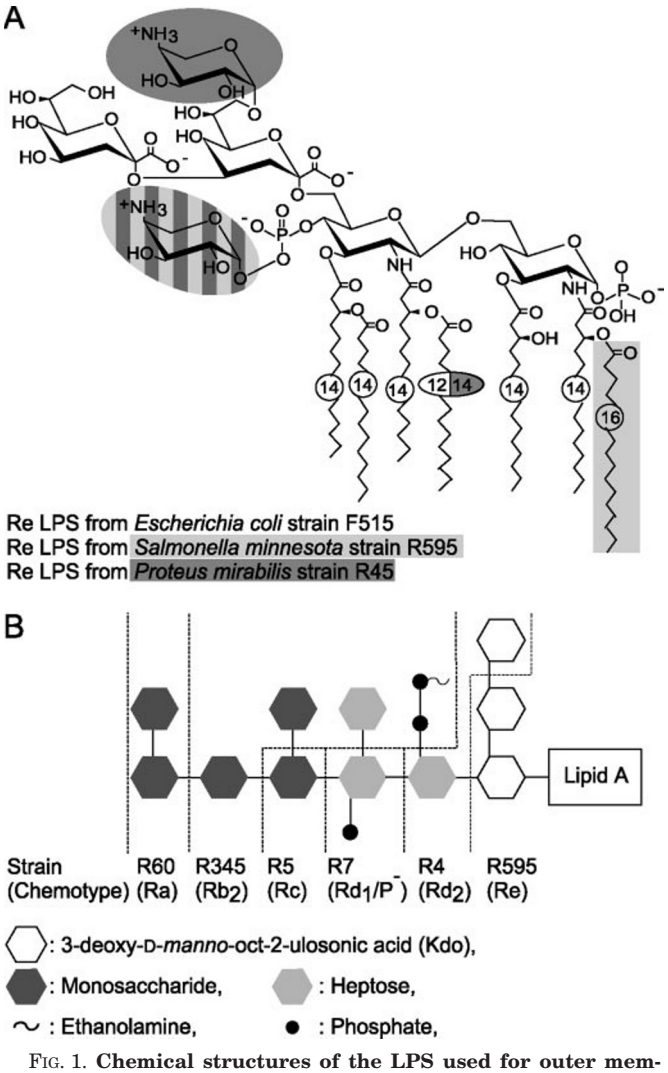

FIG. 1. **Chemical structures of the LPS used for outer membrane reconstitution.** *A*, chemical structure of Re LPS from various Gram-negative species, *i.e. E. coli* strain F515, *S. minnesota* strain R595, and *P. mirabilis* strain R45. *B*, schematic chemical structure of the core region of LPS from different rough mutant strains of *S. minnesota* and its chemotypes (*Ra* to *Re*). The phosphate residue at the second heptose and the 2-aminoethyl diphosphate residue at the first heptose are only present for the mutants R345 and R60.

In the present study, we examine the effect of the chemical structure of LPS, in particular that of the length of the core sugar moiety on the pore formation by PhoE trimers and its pore function in the OM. To this end, electrical measurements were performed on reconstituted OM as asymmetric planar membranes according to the Montal-Mueller technique. For porin from *Paracoccus denitrificans*, the role of LPS in pore formation and pore function has been shown earlier (15, 16). These authors prepared membranes from Re LPS from *S. enterica* serovar Minnesota (*S. minnesota*) strain R595 or monosaccharide-type fraction of glycosphingolipid (GSL-1), which substitutes for LPS in the OM of *Sphingomonas paucimobilis* (17), on one side and a phospholipid mixture (PL) resembling the composition of the inner leaflet on the other side. It was found that the pore formation rate in glycolipid/PL membranes was by an order of magnitude higher than in symmetric PL membranes. The influence of the length of the saccharide portion was, however, not investigated. Therefore, we then focused on the effect of the core oligosaccharide on pore formation rate of PhoE and on the voltage-dependent gating of the pores formed. Instead of LPS from *E. coli*, that from *S. minnesota,* which has a high homology to LPS from *E. coli*, was used because of the availability of a series of LPS with variable length of the sugar moiety (Fig. 1*B*).

We found that in general the pore formation rate increased with increasing length of the sugar moiety, whereas only slight differences in the pore formation rate could be observed for Re LPS from various strains. The voltage-dependent gating of PhoE pores was strongly dependent on the composition of the lipid matrix. In general, the voltage necessary for closure of PhoE was $|V_C| \geq 50$ mV. Therefore, the transmembrane voltage across the bacterial OM of $V_{OM} = 26$ mV (inside negative) (18) seems to be too low to initiate voltage-dependent closure of PhoE; however, the transmembrane voltage across the IM of $V_{IM} = 140–160$ mV (inside negative) (19) would lead to closure of accidentally incorporated porins in the IM. Thus, porin gating could be an important mechanism for self-protection of Gram-negative bacteria.

EXPERIMENTAL PROCEDURES

Lipids and Other Chemicals—Rough mutant LPS from *S. minnesota* strains R595 (LPS R595), R7 (LPS R7), R5 (LPS R5), R345 (LPS R345), R60 (LPS R60), *E. coli* strain F515 (LPS F515), and *P. mirabilis* strain R45 (LPS R45) were used in experiments with asymmetric PL/LPS membranes. The chemical structure of various Re LPS used in our experiments is shown in Fig. 1*A*, those of the core region of different chemotypes of LPS from *S. minnesota* in Fig. 1*B*. LPS was extracted by the phenol/chloroform/petroleum ether method (20) and purified, lyophilized, and transformed into the triethylamine salt form. The amount of the nonstoichiometric substitutions was analyzed by matrix-assisted laser desorption ionization time-of-flight mass spectrometry. Phosphatidylethanolamine (PE) from *E. coli*, phosphatidylglycerol (PG) from egg yolk lecithin (sodium salt), and synthetic diphosphatidylglycerol (DPG) were purchased from Avanti Polar Lipids (Alabaster, AL) and used without further purification.

LPS-free Phosphoporin PhoE from E. coli—The mature form of PhoE protein was expressed and isolated from *E. coli* strain Bl21(DE3) cells containing plasmid pCJ2 and refolded into a trypsin-resistant form as described previously (21). After refolding, the proteins were treated with trypsin (30 μg/ml) for 20 min at 37 °C followed by an incubation with 1 mM phenylmethylsulfonyl fluoride at 0 °C for 1 h to inhibit the protease. After concentration of the protein solution with centriprep 10 (Amicon, Beverly, MA, United States), the solution was dialyzed against buffer A (10 mM Tris-HCl, pH 8.0, 0.46 mM Tween 20) with 3 changes at 4 °C. Refolded proteins were further purified by anion exchange chromatography on Q-Sepharose HR (Amersham Biosciences) using a Gradifrac (Amersham Biosciences), and bound protein was eluted from the column with a linear gradient of buffer A to 0.5 M NaCl. Peak fractions containing the refolded protein were pooled and dialyzed against buffer A at 4 °C. Aliquots of protein solution (~0.5 mg/ml protein) were rapidly frozen with liquid nitrogen and stored at −20 °C. Prior to electrophoresis, samples containing refolded proteins incubated in 2% SDS-sample buffer and incubated for 10 min at room temperature, 56 °C or 100 °C, were analyzed by SDS-polyacrylamide gel electrophoresis (SDS-PAGE) as described previously (21). Refolded protein consisted mostly of heat-stable trimers (Fig. 2, *T*) with small amounts of folded monomers (Fig. 2, *m**, *lane 1*) and very low amounts of dimeric forms (Fig. 2, *D*, hardly visible in *lane 1*). Heating for 10 min at 56 °C will denature monomeric, dimeric, and small amounts of heat-unstable forms of PhoE, resulting in detection of heat-stable trimers (Fig, 2, *T*, *lane 2*). After heating for 10 min at 100 °C all forms were denatured, resulting in detection of denatured PhoE monomers (Fig. 2, *m*, *lane 3*). PhoE was diluted in aqueous solution containing 0.15 mg/ml Triton X-100 and stored at 4 °C for at least 3 days before usage.

Preparation of Planar Bilayers and Electrical Measurements—For the investigation of pore formation by PhoE and its pore function in different lipid matrices, planar bilayers according to the Montal-Mueller technique (22) were prepared as described previously (23). Briefly, asymmetric bilayers were formed by opposing two lipid monolayers, one from LPS, the other from PL, prepared on aqueous subphases (1.5 ml each) from chloroformic solutions of the lipids at a small aperture (typically 150 μm diameter) in a thin Teflon septum (12.5 μm thickness). PL is composed of PE, PG, and DPG in molar ratios of 81:17:2 resembling the phospholipid composition of the inner leaflet of the outer membrane of *S. enterica* serovar Typhimurium (24).

For electrical measurements, the planar membranes were voltage clamped via a pair of Ag/AgCl electrodes connected to the head stage of

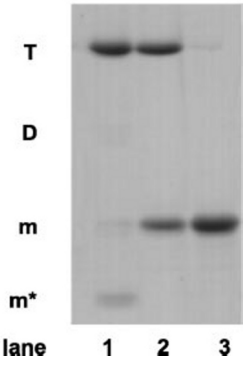

FIG. 2. **SDS-PAGE of *in vitro* folded and purified PhoE.** After folding, trypsin treatment, and purification by anion exchange chromatography, PhoE protein was analyzed by SDS-PAGE. The protein sample was dissolved in sample buffer containing 2% SDS and subsequently incubated for 10 min at room temperature (*lane 1*), 56 °C (*lane 2*), or 100 °C (*lane 3*). Proteins were stained with Coomassie Brilliant Blue R-250 after electrophoresis. The position of the trimers (*T*), dimers (*D*), denatured monomers (*m*), and folded monomers (m^*) are indicated.

a patch-clamp amplifier. In all cases the compartment opposite where the porin was added was grounded.

If not otherwise mentioned, measurements were performed at a temperature of 37 °C with subphases consisting of 100 mM KCl, 5 mM $MgCl_2$, and 5 mM HEPES adjusted to pH 7.0. The specific electrical conductivity of this bathing solution at 37 °C was 17.2 millisiemens cm^{-1}.

At the beginning of each experiment the correct membrane formation was checked by measuring membrane current and capacitance. Only membranes with a basic current of less than ±2.5 pA at a clamp voltage of ±100 mV were used for the experiments. PhoE was added to the PL side of the bilayer.

RESULTS

Pore Formation—To investigate the influence of the lipid matrix on pore formation, 20 ng PhoE were added to the PL side of various PL/LPS membranes. Fig. 3 represents a typical current trace for pore formation by PhoE added to the PL side of an asymmetric lipid bilayer with Ra LPS from *S. minnesota* strain R60 on the opposite side at a clamp voltage of 20 mV. 90 s after porin addition, the current increased stepwise. About 6 min after porin addition the pore formation rate declined, and pore formation stopped about 30 min after porin addition. The number of pores was calculated from the current traces as the quotient of membrane and single-channel current. When PhoE (up to an amount of 2 μg) was added to the LPS side of a PL/LPS membrane, no increase in membrane current was observed. Control experiments with 4.5 μg Triton X-100 showed no changes in membrane current.

The histogram of amplitudes of current steps is shown in Fig. 4 exemplarily for PL/LPS R60 membranes. The single-channel current was derived from the histogram by gauss approximation. Table I summarizes the mean current increments of single PhoE trimers in different lipid matrices. For all membranes, nearly no differences in the single-channel current were observed. Only for lipid matrices containing LPS R5 and PG slightly, but not significantly, smaller single-channel currents were determined.

The mean number of pores formed by PhoE in different lipid matrices made from PL on the side of porin addition and of rough mutant LPS from *S. minnesota* on the opposite side at a clamp voltage of 20 mV at 5, 10, 15, and 20 min after porin addition are presented in Fig. 5*A*. Each value represents the mean number of pores found in 3–5 successful experiments. Because of membrane rupture at an early stage, many experiments could not be considered. In general, membrane stability decreased with increasing length of the core sugar moiety. Furthermore, we were not successful forming stable bilayers

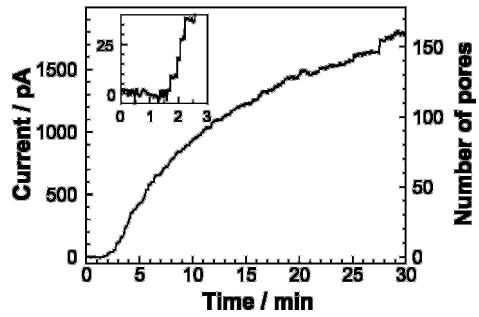

FIG. 3. **Pore formation by PhoE in PL/LPS R60 membranes.** A typical current trace at a clamp voltage of 20 mV is plotted exemplarily for LPS from *S. minnesota* strain R60. Approximately 1 to 2 min after the addition of 20 ng PhoE to the PL side of the membrane, a stepwise increase of membrane current is observed. Approximately 30 min after porin addition, pore formation ceases. The PL side consists of 81 mol% PE, 17 mol% PG, and 2 mol% DPG. The subphase contains 100 mM KCl, 5 mM $MgCl_2$ and is buffered with 5 mM HEPES. The mixture is then adjusted to a pH of 7.0 and heated to a temperature of 37 °C.

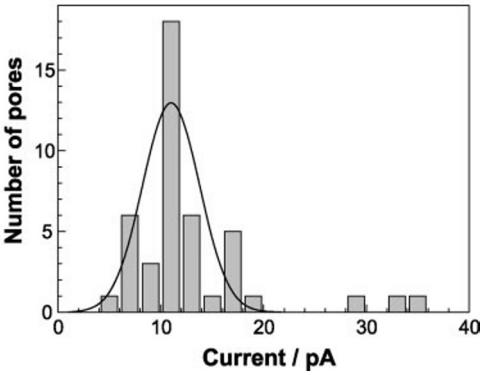

FIG. 4. **Single-channel current Λ.** The single-channel currents Λ of PhoE at a clamp voltage of 20 mV in different lipid matrices were obtained from the current traces. A typical histogram of single-channel current is plotted exemplarily for PL/LPS R60 membranes. Composition of PL side and of subphase as in Fig. 3.

using LPS from *S. minnesota* strains R4. The mean number of pores formed within 20 min decreases from LPS R60, which is set to 100%, over LPS R345 (71%), LPS R5 (16%), and LPS R7 (24%) to LPS R595 (6%). The sequence of the traces representing the data obtained with the various LPS chemotypes is the same at any time point, *i.e.* they do not cross. According to Student's *t* test, the significance level of the number of pores incorporated up to 20 min between the two most different chemotypes, LPS R60 and LPS R595, is <0.01. The corresponding significance levels between two neighboring traces are ≤ 0.61 (*e.g.* 0.61 for LPS R60 and LPS R345, 0.60 for LPS R345 and LPS R7, 0.48 for LPS R7 and LPS R5, and 0.23 for LPS R5 and LPS R595) because of the large error bars. The significance levels between more distant traces are smaller than 0.15, with the exception of the value between LPS R345 and LPS R5 (0.34).

In Fig. 5*B*, the mean numbers of PhoE pores (determined as described before) in lipid matrices composed of PL on the side of porin addition and Re LPS from various Gram-negative species (*i.e. S. minnesota* strain R595, *E. coli* strain F515, and *P. mirabilis* strain R45) on the other side are depicted. PG has been used as an example of a negatively charged phospholipid. The number of pores at 20 min decreased from 15% in the case of LPS F515, 9% (LPS R45), and 6% (LPS R595) to, in the case of PG, 2% of the values found for LPS R60. The value for symmetrical PL/PL membranes is comparable to those found for PL/PG membranes (data not shown).

Furthermore, it should be mentioned that in general the

TABLE I
Single-channel Current Λ

The single-channel currents Λ of PhoE at a clamp-voltage of 20 mV in different lipid matrices composed on the one side of PL and on the other of different chemotypes of LPS from *S. minnesota*, Re LPS from various Gram-negative species, i.e., *E. coli* strain F515, *P. mirabilis* strain R45, and PG as a charged phospholipid were obtained by gauss-approximation from the histograms of amplitudes of current steps. The error ΔΛ is given as 2 σ. Only the side opposite to porin addition is itemized. The other side was composed of PL. Composition of PL side and of subphase as in Fig. 3.

Lipid	LPS F515	LPS R45	LPS R595	LPS R7	LPS R5	LPS R345	LPS R60	PG
Λ/pA	10.8	11.2	10.6	10.0	9.0	10.4	11.2	7.6
ΔΛ/pA	5.0	3.2	5.3	1.4	5.0	7.8	2.4	5.2

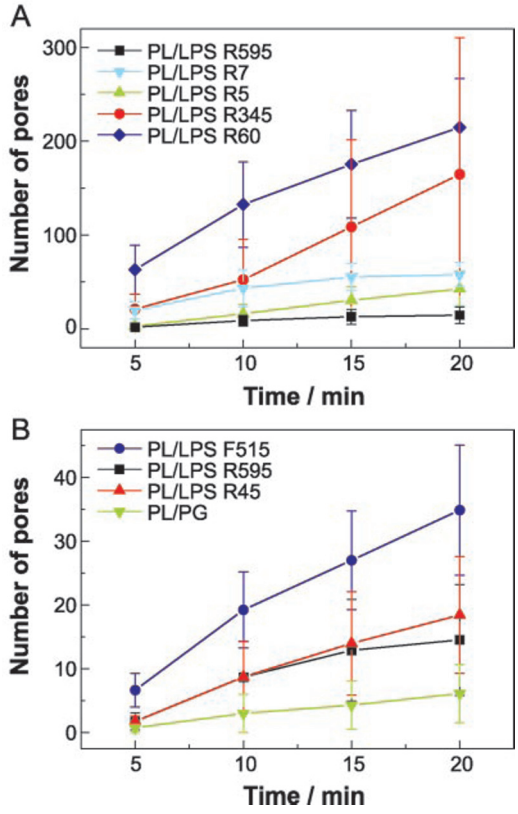

FIG. 5. **Mean number of pores.** The mean numbers of pores after addition of 20 ng PhoE were investigated in planar bilayer experiments at a clamp voltage of 20 mV for several lipid matrices composed of PL on the side of porin addition and on the other of (*A*) different chemotypes of LPS from *S. minnesota* and (*B*) Re LPS from various Gram-negative species, *i.e. E. coli* strain F515, *P. mirabilis* strain R45, and PG as a charged phospholipid. Each plotted value represents the mean current of at least three experiments. Composition of PL side and of subphase as in Fig. 3.

final number of pores reached increases from Re LPS to Ra LPS. For LPS with a short sugar moiety this finish is reached 15 to 20 min after porin addition. For LPS with a longer sugar moiety, in particular for LPS R60 and LPS R345, the maximum is reached about 20–30 min after porin addition.

The effect of the Mg^{2+} concentration on pore formation by PhoE was determined for PL/LPS F515 membranes prepared in different subphases containing 1, 5, and 15 mM $MgCl_2$, respectively. The rate of pore formation after the addition of 20 ng PhoE decreased drastically with increasing Mg^{2+} concentration (data not shown).

Pore Function—About 20 min after porin addition, the increase in membrane current ceased. To characterize the voltage-dependent closure of PhoE, current/voltage characteristics of the PhoE trimers were recorded by applying a triangular voltage (3.2 mV/s) with an amplitude of 200 mV. All curves were recorded at least twice from independent membrane preparations. The recordings were repeated several times in each experiment (until the membrane broke), and the depicted curves in Fig. 6 are in each case averages over all respective data. The plotted current is normalized to the current determined at a clamp voltage of +40 mV at which all pores were found in the open state. At small absolute clamp voltages ($|V| < 50$ mV) the membrane current was proportional to the transmembrane voltage. At higher absolute clamp voltages an underproportional increase, a steady state, or a decrease of membrane current was detected because of the closure of porin channels. The current/voltage characteristics show a hysteretic behavior. The efficiency of voltage-dependent closure can be taken from the onset and the shape of the hysteresis loops.

In Fig. 6*A* current/voltage characteristics of PhoE incorporated into different lipid bilayers made from PL on the side of porin addition and from rough mutant LPS from various *S. minnesota* strains on the other side are shown. To better distinguish between different traces the respective clamp voltages at which deviation from linearity in the positive and in the negative voltage ranges occurred because of channel closing. V_{C+} and V_{C-} are given in the figure legend. At negative clamp voltages nearly no voltage-dependent closure of the porin channels occurred. In the positive range at clamp voltages above 50 mV, a hysteretic current/voltage characteristic was observed. The efficiency of voltage-dependent closure increased with the length of the sugar portion of the LPS from LPS R595 over LPS R7 to LPS R5. In the case of LPS R345, the efficiency of voltage-dependent closure decreased in comparison to LPS R5. In the case of LPS R60, we were not able to successfully record a current/voltage characteristic because of the instability of the lipid bilayer.

In Fig. 6*B*, the current/voltage characteristics of PhoE incorporated into lipid bilayers containing Re LPS from various species (*i.e. S. minnesota* strain R595, *E. coli* strain F515, and *P. mirabilis* strain R45), PG as a negatively charged phospholipid, and PL (reconstitution of the cytoplasmic membrane) on the one side and PL on the other side are depicted. For all LPS, except that from *S. minnesota* strain R595, an effective closure of PhoE was also observed at negative clamp voltages of about −100 to −120 mV. At positive clamp voltages for LPS F515 a strong decrease in membrane current occurred. For LPS R45 and LPS R595 only a steady state was reached, and accordingly the hysteretic character of the current trace was much smaller. For both phospholipid systems effective closure of PhoE was observed in the positive voltage range. At negative clamp voltages, gating was much more pronounced in PL/PG than in PL/PL membranes, yielding almost symmetric current/voltage characteristics in the former and an asymmetric characteristic in the latter case.

DISCUSSION

In the past, several investigations have been published aiming at an understanding of the role of LPS in the biogenesis of porins. Performing *in vitro* folding studies, it has been shown that LPS is required for correct and efficient folding of PhoE into a folded monomeric intermediate (13) and that LPS influences folding and trimerization of OmpF protein (25). In the

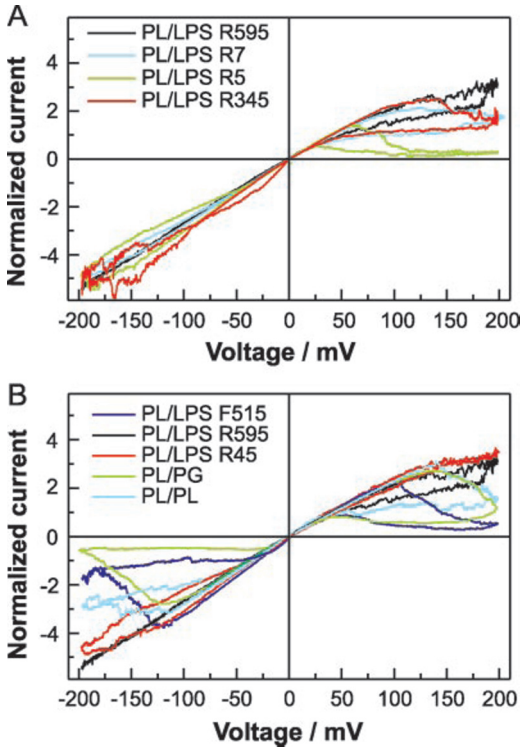

FIG. 6. **Voltage-dependent gating of PhoE.** The current/voltage-characteristics of PhoE were determined from planar bilayer experiments by applying a triangular voltage (3.2 mV/s) to asymmetric lipid matrices composed of PL on the side of porin addition and on the other of various LPS chemotypes. All *curves* were recorded at least twice from independent membrane preparations. The recordings were repeated several times in each experiment, and the depicted *curves* are in each case averages over all respective data. The current is normalized to the current determined at a clamp voltage of +40 mV. The clamp voltages V_{C+} and V_{C-} are the voltages at which deviation from linearity in the positive and in the negative voltage range, respectively, occur because of channel closing. *A*, rough mutant LPS from *S. minnesota* strains R595 (*black trace*, V_{C+} ~80 mV, $V_{C-} < -200$ mV), R7 (*cyan trace*, V_{C+} ~65 mV, V_{C-} ~−150 mV), R5 (*green trace*, V_{C+} ~60 mV, V_{C-} ~−150 mV), and R345 (*red trace*, V_{C+} ~95 mV, V_{C-} ~−145 mV). *B*, Re LPS from *E. coli* strain F515 (*blue trace*, V_{C+} ~100 mV, V_{C-} ~−110 mV), *S. minnesota* strain R595 (*black trace*, V_{C+} ~80 mV, $V_{C-} < -200$ mV), *P. mirabilis* strain R45 (*red trace*, V_{C+} ~80 mV, V_{C-} ~120 mV), PG (*green trace*, V_{C+} ~110 mV, V_{C-} ~100 mV), and PL (*cyan trace*, V_{C+} ~125 mV, V_{C-} ~−115 mV). Composition of PL side and of subphase as in Fig. 3.

present investigation we observed that the composition of the lipid bilayer, and particularly the chemical structure of LPS used for membrane reconstitution, plays an important and probably major role in the incorporation and/or late steps of pore formation by PhoE. Furthermore, we found that the electrical properties of the trimer are influenced by the composition of the lipid matrix.

It was shown previously in *in vitro* studies that the efficiency of assembly of an *in vitro* synthesized PhoE protein into the OM of different *E. coli* mutants decreases by about 95% from Ra to Re mutants (12). In that system, folding, trimerization, and insertion into the OM could not be distinguished. Subsequently it was shown that LPS was required in an early step in folding, the formation of the folded monomer (26). Re LPS was far less efficient in supporting the folding of PhoE as compared with Ra LPS (13). These monomers represent genuine intermediates since they could be trimerized into native-like trimers after incubation with OM, in which they appeared to be inserted since they could not be extracted with urea. Now we observe that the composition of the lipid matrix has a strong influence on late steps in the biogenesis, insertion, and/or pore formation of *in vitro* folded and LPS-free porin since the efficiency of pore formation by PhoE differs in lipid matrices containing different chemotypes of LPS from *S. minnesota*. In general, the number of pores incorporated at a given time decreased from Ra LPS (LPS R60) to Re LPS (LPS R595) (Fig 5*A*). The brought distribution of the mean number of pores at a given time in a particular membrane system can be explained by differences in the time for diffusion of the porins from the locus of addition to the subphase to the membrane surface in repetitive experiments. Because of the partly overlapping error bars, a quantitative correlation between pore formation and lipid composition can not be established between traces corresponding to neighboring chemotypes. However, with increasing distance between the chemotypes the significance levels decrease to $p < 0.01$ between LPS R60 and LPS R595. Therefore, from the fact that the sequence in the number of pores incorporated into the various lipid matrices was the same at any time, it can be deduced that the lipid matrix determines the efficiency of porin assembly into the OM. The presence of LPS with a longer core sugar moiety on the membrane leaflet opposite porin addition thus promotes all steps in porin assembly.

Now, as the composition of the lipid bilayer, in particular the LPS chemotype on the side opposite to porin addition, determines the pore formation rate, the question arises as to which physicochemical membrane properties are responsible for this observation. Here in the first place membrane fluidity and surface charge density have to be considered.

It has been shown earlier that an increase in membrane fluidity increases the formation of lytic membrane pores by the complement system (27). However, this parameter cannot explain the positive correlation between pore formation and the length of the core sugar moiety, because membrane fluidity varies only slightly for the LPS used in the present investigation (28). Furthermore, the least efficient pore formation was observed in PL/PG and PL/PL membranes that have the highest fluidity of all lipids used.

In the case of asymmetric PL/LPS bilayers, a potential gradient arises from the higher surface charge density on the LPS side as compared with the PL side. Thus, for the influence of the core sugar moiety on pore formation, a positive correlation between the number of negative charges and the pore formation by PhoE can be stated. LPS R60 and LPS R345, which give rise to the highest pore formation, carry at least 5 negative charges. LPS R7, LPS R5, and LPS F515, with 4 negative charges each, are in the intermediate range. LPS R595 and LPS R45, carrying less than 4 charges each, show even smaller pore formation rates. Also, the decrease in pore formation at higher Mg^{2+} concentration could be explained by a reduction of negative charges on the LPS side. However, it should be mentioned that the higher pore formation rate in PL/LPS R60 membranes compared with PL/LPS R345 membranes, as well as the same rate in PL/LPS R595 and PL/LPS R45 membranes, cannot be explained by differences in the respective LPS charges. Furthermore, it can be taken from the current/voltage characteristics that a high external potential does not induce any further pore formation (Fig. 6, *A* and *B*). This effect might be explained assuming that the potential gradient is not responsible for the differences in pore formation rates. Rather, specific interactions between the divalent cations and the negative charges at the outer side of the porin and the negative groups of the glycolipids stabilizing the porin in its functional transmembrane configuration (29, 30) are responsible for the differences in pore formation rates. These specific interactions might also explain why the number of pores found in PL/LPS R7 membranes is slightly higher than in PL/LPS R5 membranes, although the core region of the latter carries an additional glucose.

In addition to membrane fluidity and negative surface charge, several further structural parameters of LPS that might influence pore formation are known. Thus, the tendency of the lipid A portion of the LPS to form nonlamellar structures (31) might influence the stability of the LPS side of the PL/LPS bilayer. For the *S. minnesota* chemotypes, which have identical lipid A portions, membrane stability might be further reduced by the increasing length of the core sugar because of the increasing hydrophilicity of the LPS and repulsion between increasing numbers of negative charges. Within the context of membrane stability, the reduced pore formation by PhoE in PL/LPS F515 bilayers prepared in subphases containing higher amounts of Mg^{2+} can be understood on the basis of an increased membrane stability attributed to cross linking of LPS molecules by the divalent cations (4). A reduction of the stability of the LPS layer might do one of the following: (i) allow pore formation by porins already inserted into the PL side or (ii) influence the stability of the entire membrane and thus facilitate insertion and pore formation. The former possibility seems to be unlikely, because lower amounts of PhoE (10, 32) and other outer membrane proteins (11) have been found in Re mutants than in wild-type bacteria, indicating that these proteins do not insert into the membrane.

The differences in pore formation between PL/LPS R595 and PL/LPS R45 membranes on the one and PL/LPS F515 membranes (Fig. 5*B*) on the other hand can be explained by the additional 4-amino-4-deoxy-β-l-arabinose at the lipid A portion that leads to a reduction of the net negative charge from 4 to 3.5. However, the second 4-amino-4-deoxy-β-l-arabinose on the first Kdo of LPS R45, which causes a further reduction of the charge to 3, has no influence on pore formation. This might be explained by a compensation of the destabilizing contribution of the higher charge of LPS R595 by the stabilizing effect of an additional fatty acid (Fig. 1*A*).

Our findings also answer a question raised by Korteland and Lugtenberg (32). These authors had shown in *in vivo* studies that the uptake of negatively charged substrates by PhoE was more efficient in Re mutants. They stated that these findings are a consequence of one of the following: (i) an increased effective diameter of the pore (ii) an increased amount of open, functional pores or (iii) the absence of sterical hindrance by the sugar and the loss of negatively charged phosphate groups leading to reduced charge repulsion. From our data it is obvious that the diameter of the pore does not change (Table I), the number of open pores does not increase (Fig. 5), and therefore, the absence of a sterical hindrance and reduced charge repulsion seem to be more likely.

In Gram-negative bacteria, the periplasmic space is highly anionic compared with the external medium, mainly because of the anionic membrane-derived oligosaccharides. Membrane-derived oligosaccharides contribute to the Donnan potential across the outer membrane V_{OM}, which was determined for *E. coli* in the presence of an external cation concentration of 100 mM to be 26 mV (inside negative) (18). For the IM, a voltage of ~150 mV (inside negative) is discussed (19).

For all lipid matrices used in this study, the voltage required for voltage-dependent closure is $|V| > 50$ mV (Fig. 6, *A* and *B*). Thus, from our data it may be concluded that all PhoE porins incorporated into the OM are in the open state, and therefore, they have no function for the regulation of the transmembrane voltage. Interestingly, in the case of PL/PL membranes the voltage required for closure of PhoE is $\leq$125 mV in both directions, which is in the same order of magnitude as the proposed transmembrane voltage across the IM. Similar values have also been found in patch-clamp experiments on giant vesicles made from azolectin (33). Therefore, as was previously suggested (34), if trimers were missorted to the IM, pores would be closed to prevent a short circuit destroying the electrochemical potential across the IM. The IM is thus protected by the following two mechanisms: (i) the reduced pore formation in phospholipid membranes as compared with PL/LPS membranes and (ii) the voltage-dependent closure of PhoE accidentally incorporated into the IM. From the asymmetry of the current/voltage characteristics of PhoE incorporated into symmetric PL/PL membranes, a directed incorporation of the porin can be deduced as it has been discussed in more detail with the porin from *P. denitrificans* (15), very likely with extracellular loops facing outwards.

For porin from *P. denitrificans*, a correlation between the surface charge density of the glycolipid leaflet and porin gating was found when the LPS side of the membrane was at a negative potential with regard to the PL side (15, 16). These studies were, however, restricted to Re LPS and GSL-1. In Fig. 6*B* it can be seen that under the same conditions (positive voltage, *i.e.* LPS side negative) PhoE channel closing is most pronounced for LPS F515, which carries 4 negative charges, and decreases over LPS R595 to LPS R45, which carries 3 negative charges. However, for PhoE incorporated into the PL/LPS bilayers containing LPS from various strains of *S. minnesota* (Fig. 6*A*), channel closing is more efficient for PL/LPS R5 membranes followed by PL/LPS R7, and is least efficient in PL/LPS R595 membranes, given that all LPS carry 3 to 4 negative charges and the increase in negative charge from these LPS to LPS R345 does lead to a decreased gating compared with LPS R5. Furthermore, the gating was most efficient for PL/PG membranes despite the fact that the absolute value of the surface charge density is lower than for LPS R45.

Interestingly, in the positive voltage range the clamp voltage necessary to induce pore closure of PhoE in lipid bilayers containing on one side LPS from *S. minnesota* strains R595, R7, or R5 seems to decrease with increasing length of the sugar moiety. These data indicate that not only for the pore formation but also for the gating, not the surface charge density, but particular functional groups of the LPS are decisive. Specific interactions between LPS and the extracellular loops could influence their conformational changes, which according to studies using atomic force microscopy are involved in the gating process (35).

For negative clamp voltages down to −200 mV for all membranes made from LPS from *S. minnesota*, almost no voltage-dependent closure can be seen. This observation is in complete contrast to the data obtained for LPS F515, LPS R45, and PG showing a pronounced closing in the negative voltage range (Fig. 6*B*). This effect might be explained by mechanical stress caused by the additional fatty acid of LPS from *S. minnesota* compared with that from *E. coli*. An influence of the acyl chain region of the lipid matrix on porin gating has also been observed for porin from *P. denitrificans* (15) where gating was completely inhibited at temperatures below the phase transition temperature of the LPS. Thus, the additional fatty acid may have a similar effect on the porin channel as acyl chain rigidification.

Our data clearly emphasize the role of LPS in pore formation by and function of PhoE. In particular, from the qualitatively different incorporation rates it can be deduced that LPS is the parameter governing the formation of porin channels in the reconstituted OM and that no particular insertion sites are required and, thus, LPS has an important function for the late steps in porin biogenesis. The LPS chemical structure does, however, not only influence pore formation, but also channel gating. Thus, it is of unique importance to consider the asym-

metric composition of the OM of Gram-negative bacteria with LPS on one side and PL on the other side when aiming at the determination of porin function in reconstitution systems.

REFERENCES

1. Lugtenberg, B., and Van Alphen, L. (1983) *Biochim. Biophys. Acta* **737,** 51–115
2. Rietschel, E. Th., Kirikae, T., Schade, F. U., Mamat, U., Schmidt, G., Loppnow, H., Ulmer, A. J., Zähringer, U., Seydel, U., Di Padova, F., Schreier, M., and Brade, H. (1994) *FASEB J.* **8,** 217–225
3. Holst, O. (1999) in *Endotoxin in Health and Disease* (Brade, H., Opal, S. M., Vogel, S. N., and Morrison, D. C., eds) pp. 115–154, Marcel Dekker, Inc., New York
4. Nikaido, H., and Vaara, M. (1985) *Microbiol. Rev.* **49,** 1–32
5. Overbeeke, N., and Lugtenberg, B. (1980) *FEBS Lett.* **112,** 229–232
6. Benz, R., and Bauer, K. (1988) *Eur. J. Biochem.* **176,** 1–19
7. Cowan, S. W., Schirmer, T., Rummel, G., Steiert, M., Ghosh, R., Pauptit, R. A., Jansonius, J. N., and Rosenbusch, J. P. (1992) *Nature* **358,** 727–733
8. Bernstein, H. D. (2000) *Curr. Opin. Microbiol.* **3,** 203–209
9. Schatz, P. J., and Beckwith, J. (1990) *Annu. Rev. Genet.* **24,** 215–248
10. Tommassen, J., and Lugtenberg, B. (1981) *J. Bacteriol.* **147,** 118–123
11. Ames, G. F. L., Spudich, E. N., and Nikaido, H. (1974) *J. Bacteriol.* **117,** 406–416
12. De Cock, H., van Blokland, S., and Tommassen, J. (1996) *J. Biol. Chem.* **271,** 12885–12890
13. De Cock, H., Brandenburg, K., Wiese, A., Holst, O., and Seydel, U. (1999) *J. Biol. Chem.* **274,** 5114–5119
14. Sen, K., and Nikaido, H. (1991) *J. Bacteriol.* **173,** 926–928
15. Wiese, A., Schröder, G., Brandenburg, K., Hirsch, A., Welte, W., and Seydel, U. (1994) *Biochim. Biophys. Acta* **1190,** 231–242
16. Wiese, A., Reiners, J. O., Brandenburg, K., Kawahara, K., Zähringer, U., and Seydel, U. (1996) *Biophys. J.* **70,** 321–329
17. Kawahara, K., Matsuura, M., and Danbara, H. (1990) *Jpn. J. Med. Sci. Biol.* **43,** 250
18. Sen, K., Hellman, J., and Nikaido, H. (1988) *J. Biol. Chem.* **263,** 1182–1187
19. Bakker, E. P., and Mangerich, W. E. (1981) *J. Bacteriol.* **147,** 820–826
20. Galanos, C., Lüderitz, O., and Westphal, O. (1969) *Eur. J. Biochem.* **9,** 245–249
21. Jansen, C., Heutink, M., Tommassen, J., and De Cock, H. (2000) *Eur. J. Biochem.* **267,** 3792–3800
22. Montal, M., and Mueller, P. (1972) *Proc. Natl. Acad. Sci. U. S. A.* **69,** 3561–3566
23. Wiese, A., and Seydel, U. (2000) *Methods Mol. Biol.* **145,** 355–370
24. Osborn, M. J., Gander, J. E., Parisi, E., and Carson, J. (1972) *J. Biol. Chem.* **247,** 3962–3972
25. Sen, K., and Nikaido, H. (1991) *J. Biol. Chem.* **266,** 11295–11300
26. De Cock, H., and Tommassen, J. (1996) *EMBO J.* **15,** 5567–5573
27. Wiese, A., Grünewald, P., Schaper, K. J., and Seydel, U. (2001) *J. Endotoxin Res.* **7,** 147–155
28. Brandenburg, K., Kusumoto, S., and Seydel, U. (1997) *Biochim. Biophys. Acta* **1329,** 183–201
29. Weiss, M. S., Abele, U., Weckesser, J., Welte, W., Schiltz, E., and Schulz, G. E. (1991) *Science* **254,** 1627–1630
30. Weiss, M. S., and Schulz, G. E. (1992) *J. Mol. Biol.* **227,** 493–509
31. Brandenburg, K., Richter, W., Koch, M. H. J., Meyer, H. W., and Seydel, U. (1998) *Chem. Phys. Lipids* **91,** 53–69
32. Korteland, J., and Lugtenberg, B. (1984) *Biochim. Biophys. Acta* **774,** 119–126
33. Berrier, C., Besnard, M., and Ghazi, A. (1997) *J. Membr. Biol.* **156,** 105–115
34. Eppens, E. F., Saint, N., Van Gelder, P., van Boxtel, R., and Tommassen, J. (1997) *FEBS Lett.* **415,** 317–320
35. Müller, D. J., and Engel, A. (1999) *J. Mol. Biol.* **285,** 1347–1351